Organometallics **1985**, *4*, 1048–1053

identified by ^{1}H NMR. The residue in each case was a viscous oil.

1-(Trimethylsilyl)-2-(bromodimethylstannyl)ethane (contaminated with ca. 5% (NMR) 1-(trimethylsilyl)-1-(bromodimethylstannyl)ethane): bp 58–60 °C (10^{-2} torr); ^{1}H NMR ($CDCl_3$) δ 0.02 (s, 9 H, $SiMe_3$); 0.72 (s, 6 H, ^{2}J(SnH) = 54 Hz, Br Me_2Sn); ^{13}C NMR ($CDCl_3$) δ −2.42 (^{1}J(SnC) = 319.0 Hz, $SnMe_2Br$), −2.31 (^{1}J(SiC) = 51.0 Hz, $SiMe_3$), 11.20 (^{1}J(SnC) = 391.2 Hz, $SnCH_2$), 11.61 (^{2}J(SnC) = 41.1 Hz, $SiCH_2$); ^{29}Si NMR ($CDCl_3$) δ 2.80 (^{3}J(^{29}Si–^{119}Sn) = 143.6 Hz) [impurity: δ 4.53 (^{2}J(SiSn) = 4 Hz)]; ^{119}Sn NMR ($CDCl_3$) δ 141.90 [impurity: δ 152.15]. Anal. Calcd for $C_7H_{19}BrSiSn$: C, 25.5; H, 5.8. Found: C, 25.5; H, 5.6.

1,2-Bis(bromodimethylstannyl)ethane (contaminated with ca. 40% 1,1-bis(bromodimethylstannyl)ethane): ^{1}H NMR ($CDCl_3$) δ 0.80 (s, 12 H, ^{2}J(SnH) = 54 Hz, $BrMe_2Sn$), 1.67 (s, 4 H, ^{3}J(SnH) = 88 Hz, CH_2); ^{13}C NMR ($CDCl_3$) δ −1.73 (^{1}J(SnC) = 331.3 Hz, $BrMe_2Sn$), 14.17 (^{1}J(SnC) = 366.8, ^{2}J(SnC) = 40.5 Hz, CH_2) [impurity: δ −0.71 (^{1}J(SnC) = 354.0 Hz, $BrMe_2Sn$), 13.51 (^{2}J(SnC) = 27.7 Hz, CH_3), 15.84 (^{1}J(SnC) = 308.5 Hz, $CHSn_2$); ^{119}Sn NMR ($CDCl_3$) δ 137.3 (^{3}J(^{119}Sn–^{119}Sn) = 1558 Hz) [impurity: δ 147.4 (^{2}J(SnSn) = 46.4 Hz)]. Fractional crystallization yielded the pure 1,2-isomer, mp 123–126 °C. Anal. Calcd for $C_6H_{16}Br_2Sn_2$: C, 14.8; H, 3.3. Found: C, 15.0; H, 3.3.

1-(Trimethylsilyl)-1,2-bis(bromodimethylstannyl)ethane (contaminated with ca. 12% 1-(trimethylsilyl)-1,1-bis(bromodimethylstannyl)ethane): bp 140 °C (10^{-3} torr); ^{1}H NMR ($CDCl_3$) δ 0.15 (s, 9 H, $SiMe_3$), 0.78 (s, 6 H, ^{2}J(SnH) = 52 Hz, $BrMe_2Sn$); ^{13}C NMR ($CDCl_3$) δ −1.04 (^{1}J(SiC) = 52.1, ^{3}J(CSiCSn) = 19.1 Hz, $SiMe_3$), −0.27 (^{1}J(SnC) = 324.2 Hz, $BrMe_2Sn$), 0.49 (^{1}J(SnC) = 358.6 Hz, $BrMe_2Sn$), 17.09 (^{1}J(SnC) = 268.3, ^{2}J(SnC) = 40.4 Hz, CH_2), 18.05 (^{1}J(SnC) = 390.5, ^{2}J(SnC) = 38.1 Hz, CH); ^{29}Si NMR ($CDCl_3$) δ 4.20 (^{3}J(SiSn) = 101.4, ^{2}J(SiSn) = 5.4 Hz [impurity: δ 6.34 (^{2}J(SiSn) = 18 Hz]; ^{119}Sn NMR ($CDCl_3$) δ 113.8, 162.3 (^{3}J(^{119}Sn–^{119}Sn) = 400.5 Hz) [impurity: δ 139.9 (^{2}J(^{119}Sn–^{119}Sn) = 191.5 Hz)].

Acknowledgment. We thank the Deutsche Forschungsgemeinschaft and the Fonds der Chemischen Industrie for supporting this work.

Registry No. **1**, 96130-34-6; **2**, 56580-70-2; **3**, 96130-35-7; **4**, 60041-25-0; **5**, 96130-36-8; **6**, 96130-37-9; **7**, 96130-38-0; **8**, 96130-39-1; **9**, 96130-40-4; **10**, 96130-41-5; **11**, 96130-42-6; $Me_3SiC(SnMe_3){=}CH_2$, 87241-31-4; $(Me_3Sn)_2C{=}CH_2$, 87673-34-5; *t*-$BuC(SnMe_3){=}CH_2$, 96130-43-7; $PhC(SnMe_3){=}CH_2$, 1198-01-2; (*E*)-$Me_3SnCH{=}CH$-*t*-Bu, 96130-44-8; $Me_3SiCH{=}CH_2$, 754-05-2; Me_3SnH, 1631-73-8; $Me_3SnCH{=}CH_2$, 754-06-3; $BrMe_2SnCH_2CH_2SnMe_2Br$, 96130-45-9; $BrMe_2SnCH_2CH_2SiMe_3$, 96130-46-0; $Me_3SiCH(SnMe_2Br)CH_2SnMe_2Br$, 96130-47-1; Me_2SnBr_2, 2767-47-7; $Me_3SiCBr{=}CH_2$, 13683-41-5; Me_3SnCl, 1066-45-1; 1-(trimethylsilyl)-1-(bromodimethylstannyl)ethane, 96130-48-2; 1,1-bis(bromodimethylstannyl)ethane, 96130-49-3; 1-(trimethylsilyl)-1,1-bis(bromodimethylstannyl)ethane, 96130-50-6.

Generation and Decomposition of $M'MCp_2^+$ (M′, M = Fe, Co, Ni; Cp = Cyclopentadienyl) in the Gas Phase

D. B. Jacobson[†] and B. S. Freiser*

Department of Chemistry, Purdue University, West Lafayette, Indiana 47907

Received July 31, 1984

$M'L^+$ (M′ = Fe, Co, Ni; L = isobutene, butadiene) react with ferrocene and nickelocene in the gas phase yielding predominantly the mixed-metal metallocenes $M'MCp_2^+$ by ligand displacement. $CoNiCp_2^+$ and $FeNiCp_2^+$, generated from nickelocene, undergo collisional activation to yield predominantly the metal-switching products $CoCp_2^+$ and $FeCp_2^+$, respectively. Collisional activation of $CoFeCp_2^+$, generated from ferrocene, yields both the metal switching product $CoCp_2^+$ as well as $FeCp_2^+$ in significant amounts. These mixed-metal metallocenes $M'MCp_2^+$ react rapidly with nickelocene and ferrocene to form condensation products. CID on the condensation products suggests that the initial $M'MCp_2^+$ unit maintains its integrity with the added metallocene coordinated loosely to the $M'MCp_2^+$ unit. Finally, limits are obtained for the ionization potentials, heats of formation, and metal–metallocene bond energies of the mixed-metal metallocenes.

Introduction

Recently, we reported a novel metal-switching reaction[1] in the gas phase involving the reaction of Ti^+ and Rh^+ with ferrocene and nickelocene (process 1).[2] The only competing process was simple charge transfer (reaction 2). In addition, V^+ and Y^+ are also observed to undergo metal switching (reaction 1).[3] The ionization potential (IP) of the reacting metal ion appears to be the critical parameter for observing metal switching. For example, only process 2 occurs for M′ = Fe, Co, and Ni which unlike Rh, Ti, V, and Y have IP's well above ferrocene and nickelocene.[4] Metal switching, process 1, proceeds by initial formation of an activated $M'MCp_2^+$ species which decomposes by elimination of the native metal. Charge transfer may proceed both by initial formation of $M'MCp_2^+$ which eliminates the invading metal or by long-range charge transfer.

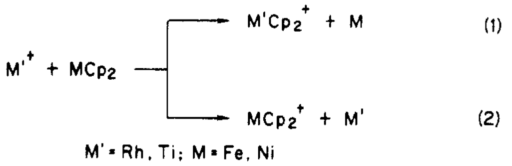

Stable $M'MCp_2^+$ ions may be generated by reaction 3 where displacement of the ligand, L, stabilizes the

---

[†] Department of Chemistry, California Institute of Technology, Pasadena, CA 91125.

(1) Jacobson, D. B.; Byrd, G. D.; Freiser, B. S. *J. Am. Chem. Soc.* **1982**, *104*, 2320.

(2) Throughout this paper, "Cp" refers to cyclopentadienyl.

(3) Jacobson, D. B.; Freiser, B. S., unpublished results.

(4) Ionization potential (IP) of Fe = 7.87 eV, Co = 7.86 eV, and Ni = 7.64 eV from: Rosenstock, H. M.; Draxl, K.; Steiner, B. W.; Herron, J. T. *J. Phys. Chem. Ref. Data, Suppl.* **1977**, *6*. IP($FeCp_2$) = 6.88 ± 0.1 eV, IP($CoCp_2$) = 5.56 ± 0.1 eV, IP($NiCp_2$) = 6.51 ± 0.1 eV from: Green, J. C. *Struct. Bonding (Berlin)* **1981**, *43*, 37.

0276-7333/85/2304-1048\$01.50/0

$M'MCp_2^+$ species. Decomposition of the bimetallic species

$$M'L^+ + MCp_2 \rightarrow M'MCp_2^+ + L \qquad (3)$$

generated in reaction 3 by collision-induced dissociation (CID) yields useful information on the nature of these ions. In this paper we report the generation of stable $M'MCp_2^+$ ions (M′ = Fe, Co, Ni; M = Fe, Ni) in the gas phase by reaction of (olefin)metal ions with ferrocene and nickelocene using Fourier transform mass spectrometry (FTMS). The chemistry of these novel bimetallic species was probed by studying their decomposition pathways and reactivity.

Experimental Section

The theory, instrumentation, and methodology of ion cyclotron resonance (ICR) spectrometry[5] and Fourier transform mass spectrometry (FTMS)[6] have been discussed at length elsewhere. All experiments were performed by using a prototype Nicolet FTMS-1000 Fourier transform mass spectrometer previously described in detail[7,8] and equipped with a 5.2-cm cubic trapping cell situated between the poles of a Varian 15-in. electromagnetic maintained at 0.9 T. The cell was constructed in our laboratory and includes a $^1/_4$-in. diameter hole in one of the transmitter plates which permits irradiation with various light sources. High-purity foils of the appropriate metals were supported on the opposite transmitter plate. Metal ions were generated by focusing the beam of a Quanta Ray Nd:YAG laser (frequency doubled to 530 nm) onto the metal foils. Details of the laser ionization technique have been described elsewhere.[9] Experimental conditions were adjusted to minimize complications due to excited state metal ions.[9c] We cannot rule out the possibility, however, that a small abundance of these species were present.

Chemicals were obtained commercially (except for nickelocene and cyclopentadienyliron dicarbonyl dimer) and used as supplied. Nickelocene[10] and cyclopentadienyliron dicarbonyl dimer[11] were prepared by standard techniques and purified by multiple sublimations and recrystalizations, respectively. No impurities were evident in their electron-impact mass spectra. Sample pressures were on the order of 5×10^{-8} torr. A Baynard–Alpert ionization gauge was used to monitor pressure.

M(isobutene)$^{+}$[12] and M(butadiene)$^{+}$[13,14] ions were generated by reactions 4 and 5, respectively. Since FTMS is a single region mass spectrometer, all reagent gases are present in the same chamber. As a result, studying the chemistry of product ions with specific reagent gases can be complicated by reactions with the parent neutral gas. Addition of reagent gases through a pulsed valve can alleviate this problem.[15] Both neopentane and 1-butene were introduced into the vacuum chamber through a General Valve Corp. Series 9 pulsed solenoid valve and were pumped away in ~250 ms. Hence, reactions of $M(C_4H_8)^+$ and $M(C_4H_6)^+$ with metallocenes could be studied vs. time without complications due to competing reactions.

$$M^+ + \text{neopentane} \rightarrow MC_4H_8^+ + CH_4 \qquad (4)$$

$$M^+ + \text{1-butene} \rightarrow MC_4H_6^+ + H_2 \qquad (5)$$

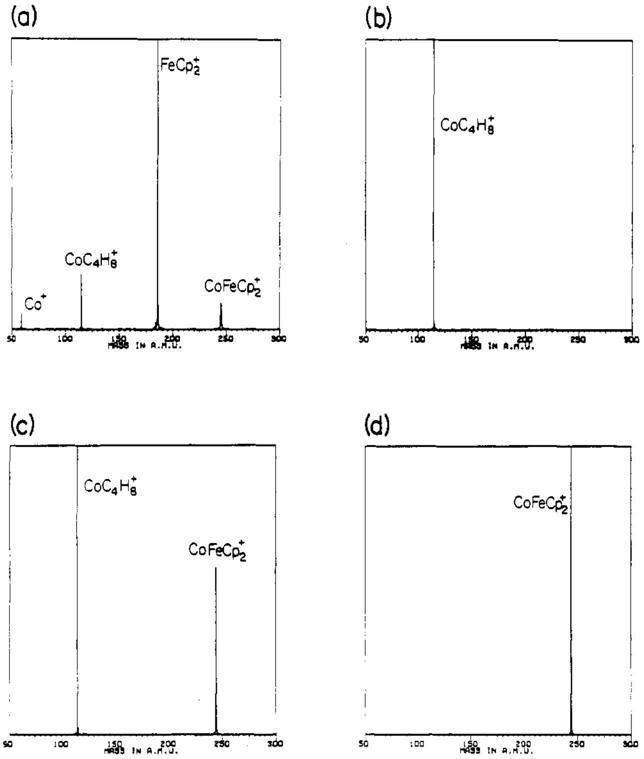

Figure 1. (a) Mass spectrum obtained when laser desorbed Co$^+$ is allowed to react with neopentane (pulsed into the vacuum chamber) and ferrocene at ~5×10^{-8} torr static pressure for 400 ms. The large abundance of $FeCp_2^+$ is formed predominantly in the laser plasma by desorption/ionization of ferrocene adsorbed on the metal surface and not by a gas-phase ion–molecule reaction. (b) Same as a except $CoC_4H_8^+$ has been isolated by swept double-resonance pulses. (c) Same as b except a 500 ms trap follows isolation of $CoC_4H_8^+$ allowing it to interact with ferrocene. (d) Same as c except $CoFeCp_2^+$ is isolated. All spectra are normalized to the most intense peak.

The metal–ligand species generated in reactions 4 and 5 were isolated by swept double-resonance ejection techniques.[6] A 400-ms delay prior to isolation allowed all the pulsed hydrocarbon reagent to be pumped away. Figure 1 illustrates the mass spectra obtained when Co$^+$ is trapped in the presence of neopentane (pulsed into the instrument) and ferrocene. The large abundance of $FeCp_2^+$ in Figure 1a is generated predominantly in the laser plasma by desorption/ionization of ferrocene adsorbed on the metal surface and not by gas-phase ion–molecule reactions. The $CoC_4H_8^+$ ions are isolated (Figure 1b) and allowed to react with ferrocene (Figure 1c). Additional swept ejection pulses can be used to isolate the $CoFeCp_2^+$ ions (Figure 1d) so both its reactivity and CID processes can be studied.

Details of the collision-induced dissociation (CID) experiments have previously been discussed.[7,8,14] Argon was used as the collision gas at a pressure of 5×10^{-6} torr. The collision energy of the ions can be varied (typically between 0 and 100 eV) from which plots of CID product ion intensities vs. kinetic energy can be made. These plots are reproducible to ±5% absolute and are informative, yielding additional structural and mechanistic information. The spread in ion kinetic energies is dependent on the total average kinetic energy and is approximately 35% at 1 eV, 10% at 10 eV, and 5% at 30 eV.[16]

---

(5) For reviews on ICR see: (a) Beauchamp, J. L. *Annu. Rev. Phys. Chem.* **1971**, *22*, 527. (b) Lehman, T. A.; Bursey, M. M. "Ion Cyclotron Resonance Spectrometry"; Wiley-Interscience: New York, 1976.

(6) (a) Comisarow, M. B.; Marshall, A. G. *Chem. Phys. Lett.* **1974**, *26*, 489. (b) Comisarow, M. B.; Grassi, V.; Parisod, G. *Chem. Phys. Lett.* **1978**, *57*, 413. (c) Marshall, A. G.; Comisarow, M. B. *J. Chem. Phys.* **1979**, *71*, 4434. (d) Ghaderi, S.; Kulkarni, P. S.; Ledford, E. B.; Wilkins, C. L.; Gross, M. L. *Anal. Chem.* **1981**, *53*, 428.

(7) (a) Cody, R. B.; Freiser, B. S. *Int. J. Mass Spectrom. Ion Phys.* **1982**, *41*, 199. (b) Cody, R. B.; Burnier, R. C.; Freiser, B. S. *Anal. Chem.* **1982**, *54*, 96.

(8) Burnier, R. C.; Cody, R. B.; Freiser, B. S. *J. Am. Chem. Soc.* **1982**, *104*, 7436.

(9) (a) Cody, R. B.; Burnier, R. C.; Reents, W. D., Jr.; Carlin, T. J.; McCrery, D. A.; Freiser, B. S. *Int. J. Mass Spectrom. Ion Phys.* **1980**, *33*, 37. (b) Burnier, R. C.; Byrd, G. D.; Freiser, B. S. *J. Am. Chem. Soc.* **1981**, *103*, 4360. (c) Cassady, C. J. Ph.D. Thesis, Purdue University, 1984.

(10) Barnett, K. *J. Chem. Educ.* **1974**, *51*, 422.

(11) Angelici, R. J. "Synthesis and Technique in Inorganic Chemistry"; W. Saunders: London, 1969; p 135.

(12) Structural studies on $MC_4H_8^+$ (M = Fe, Co, Ni) formed in reaction 4 indicate formation of M(isobutene)$^+$, see: (a) Jacobson, D. B.; Freiser, B. S. *J. Am. Chem. Soc.* **1983**, *105*, 5197. (b) Larsen, B. S.; Ridge, D. P. *J. Am. Chem. Soc.* **1984**, *106*, 1912.

(13) Armentrout, P. B.; Halle, L. F.; Beauchamp, J. L. *J. Am. Chem. Soc.* **1981**, *103*, 6624.

(14) Jacobson, D. B.; Freiser, B. S. *J. Am. Chem. Soc.* **1983**, *105*, 7484.

(15) A detailed description of pulsed valve introduction of reagent gases in conjunction with FTMS can be found in: Carlin, T. J.; Freiser, B. S. *Anal. Chem.* **1983**, *55*, 571.

(16) Huntress, W. T.; Mosesman, M. M.; Elleman, D. D. *J. Chem. Phys.* **1971**, *54*, 843.

Table I. Distribution of Ions Resulting from the Primary Reactions of $M(C_4H_8)^+$ and $M(C_4H_6)^+$ with Ferrocene and Nickelocene

		ion, %					
metallocene (M)	ion (M′)	MCp_2^+	$M'Cp_2^+$	$M'MCp_2^+$	$M'MCp_2C_4H_4^+$	$M'MCp_2C_4H_2^+$	$M'Cp_2C_4H_2^+$
$FeCp_2$	$FeC_4H_8^+$	30		70			
	$CoC_4H_8^+$	3	3	94			
	$NiC_4H_8^+$	13		87			
$NiCp_2$	$FeC_4H_8^+$	11	44	45			
	$CoC_4H_8^+$	15	56	29			
	$NiC_4H_8^+$	47		53			
$FeCp_2$	$FeC_4H_6^+$	29		37	34		
	$CoC_4H_6^+$	5	5	46	44		
	$NiC_4H_6^+$	25		66	9		
$NiCp_2$	$FeC_4H_6^+$	21	7	72			
	$CoC_4H_6^+$	13	50	13	8	12	4
	$NiC_4H_6^+$	43		47	6	4	

Results

Primary Reactions. The results for the primary reactions of ML^+ (M = Fe, Co, Ni; L = isobutene, butadiene) with ferrocene and nickelocene are summarized in Table I. Reactions of $M(C_4H_8)^+$ with the metallocenes yields ligand displacement (reaction 6), metal switching (reaction 7), and formally charge transfer (reaction 8). Ligand displacement forming $M'MCp_2^+$ dominates for reactions with ferrocene while both ligand displacement and metal switching are prominent with nickelocene. The charge-exchange reactions (9) and (10) may occur either with

$$FeC_4H_8^+ + FeCp_2 \rightarrow FeCp_2^+ + (FeC_4H_8) \qquad (9)$$

$$NiC_4H_8^+ + NiCp_2 \rightarrow NiCp_2^+ + (NiC_4H_8) \qquad (10)$$

exchange of the metal (metal switching) or with retention of the metal. Double-resonance experiments involving isolation of naturally occurring isotopes of the metals indicate that these reactions proceed with retention of the original metallocene metal and thus by a simple charge transfer as opposed to by metal switching. Observation of reaction 7, however, suggests that reaction 8 will not always proceed by simple charge transfer.

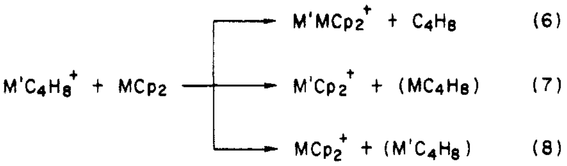

$MC_4H_6^+$ yields not only the processes outlined above for $MC_4H_8^+$ (reactions 11–13) but also a variety of dehydrogenation products as well. A significant amount of H_2 elimination, for example, occurs for reaction of $MC_4H_6^+$ with ferrocene (process 14). In addition, $MC_4H_6^+$ (M =

$$MC_4H_6^+ + FeCp_2 \rightarrow MFeCp_2C_4H_4^+ + H_2 \qquad (14)$$

Co, Ni) yields elimination of H_2 and $2H_2$ with nickelocene (reactions 15 and 16) with some $Co(Cp)_2C_4H_2^+$ also observed. $FeC_4H_6^+$ and $NiC_4H_6^+$ also yield simple charge transfer with ferrocene and nickelocene, respectively. These reactions do not proceed by metal switching in analogy to reactions 9 and 10 described above for $FeC_4H_8^+$ and $NiC_4H_8^+$.

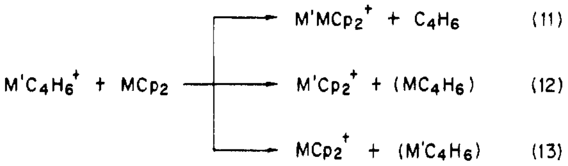

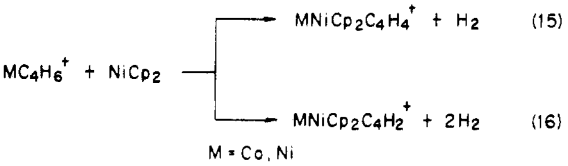

Secondary Reactions. The only process observed for $Ni_2Cp_2^+$ and $Fe_2Cp_2^+$ (formed by reactions 6 and 11) with nickelocene and ferrocene, respectively, is rapid condensation (reactions 17 and 18). Nickel transfer is the only

$$Ni_2Cp_2^+ + NiCp_2 \rightarrow Ni_3Cp_4^+ \qquad (17)$$

$$Fe_2Cp_2^+ + FeCp_2 \rightarrow Fe_3Cp_4^+ \qquad (18)$$

process observed for $CoNiCp_2^+$ (formed in reactions 6 and 11) with nickelocene (process 19). $FeNiCp_2^+$, generated

$$CoNiCp_2^+ + NiCp_2 \rightarrow CoCp_2^+ + (Ni_2Cp_2) \qquad (19)$$

in reactions 6 and 11, yields three products with nickelocene (reactions 20–22). The product of reaction 21 reacts further with nickelocene yielding $Ni_3Cp_4^+$ in analogy to reaction 17. $NiFeCp_2^+$, generated by reactions 6 and 11, produces two products with ferrocene (reactions 23 and 24). Finally, $CoFeCp_2^+$, generated by reactions 6 and 11, yields three products with ferrocene (reactions 25–27).

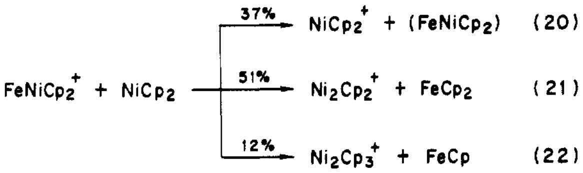

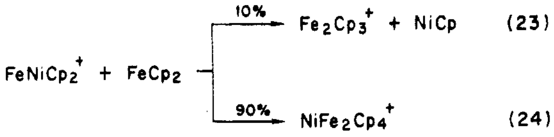

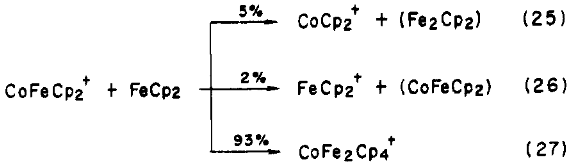

The products of reactions 17–20 and 22–27 are unreactive with the precursor metallocene. In addition, $FeCp_2^+$, $CoCp_2^+$, and $NiCp_2^+$ were also found to be inert toward ferrocene and nickelocene.[17]

---

(17) Earlier studies on the gas-phase chemistry of ferrocene and nickelocene found both $FeCp_2^+$ and $NiCp_2^+$ to be inert toward the parent metallocene. See, for example: (a) Foster, M. S.; Beauchamp, J. L. *J. Am. Chem. Soc.* **1975**, *97*, 4814. (b) Corderman, R. R.; Beauchamp, J. L. *Inorg. Chem.* **1976**, *15*, 665.

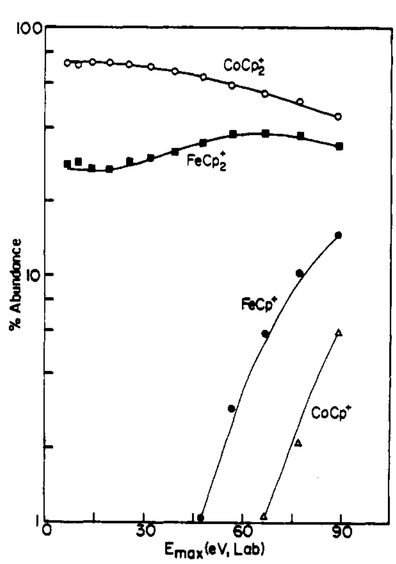

Figure 2. Variation of CID product ion intensities as a function of kinetic energy for $CoFeCp_2^+$ formed by reaction of $CoC_4H_8^+$ with ferrocene.

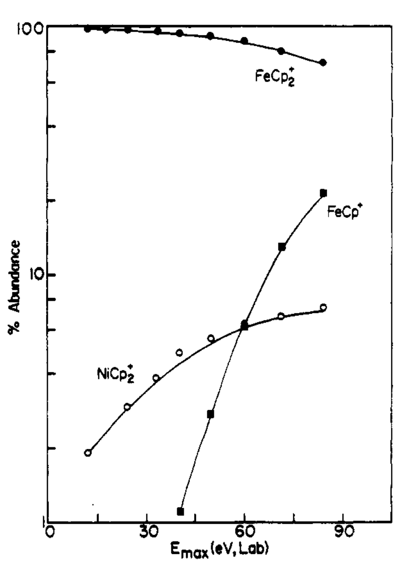

Figure 3. Variation of CID product ion intensities as a function of kinetic energy for $FeNiCp_2^+$ generated by reaction of $FeC_4H_8^+$ with nickelocene.

Decomposition of $M'MCp_2^+$. Collisional activation (CID) of $CoFeCp_2^+$, generated in reactions 6 and 11, yields $CoCp_2^+$ and $FeCp_2^+$ exclusively at low kinetic energy with some $CoCp^+$ and $FeCp^+$ formed at high kinetic energy. The variation of fragment ion abundances as a function of kinetic energy for CID of $CoFeCp_2^+$ generated by reaction of $CoC_4H_8^+$ with ferrocene is illustrated in Figure 2 and is identical (same peaks, intensities, and energy dependence within experimental error) with CID of $CoFeCp_2^+$ formed in reaction 11.

Collisional activation of $FeNiCp_2^+$, produced in reactions 6 and 11, yields predominantly $FeCp_2^+$ with some $NiCp_2^+$ and $FeCp^+$. A plot of fragment ion abundances vs. kinetic energy for CID of $FeNiCp_2^+$ generated by reaction of $FeC_4H_8^+$ with nickelocene is shown in Figure 3 and is identical (within experimental error) with CID of $FeNiCp_2^+$ formed from $FeC_4H_6^+$ with nickelocene and from $NiC_4H_8^+$ and $NiC_4H_6^+$ with ferrocene.

CID of $CoNiCp_2^+$, generated in reactions 6 and 11, yields exclusively $CoCp_2^+$ in high efficiency at low kinetic energy with a small amount of $CoCp^+$ generated at high kinetic energy with *no* $NiCp_2^+$ observed.

$Fe_2Cp_2^+$, produced in reactions 6 and 11 and by 15-eV electron impact on $[FeCp(CO)_2]_2$, yields identical CID spectra with $FeCp_2^+$ produced in high efficiency at low kinetic energy and with a small amount of $FeCp^+$ produced at high kinetic energy.

CID of $Ni_2Cp_2^+$, generated in reactions 6, 11, and 28,[18]

$$NiCp^+ + NiCp_2 \rightarrow Ni_2Cp_2^+ + Cp \qquad (28)$$

yield similar results to CID of $Fe_2Cp_2^+$ described above, with $NiCp_2^+$ being the dominant fragment and only a small amount of $NiCp^+$ observed at high kinetic energy. CID of $^{58}Ni^{60}NiCp_2^+$, generated in reaction 29, yields essentially equal amounts of $^{58}NiCp_2^+$ and $^{60}NiCp_2^+$.

$$^{58}NiC_4H_8^+ + NiCp_2 \left\{ \begin{array}{ll} \rightarrow {}^{58}Ni^{60}NiCp_2^+ + C_4H_8 & (29) \\ \rightarrow {}^{58}Ni^{58}NiCp_2^+ + C_4H_8 & (30) \end{array} \right.$$

Decomposition of $M'MCp_2L^+$. Collisional activation (CID) of $CoFeCp_2C_4H_4^+$, generated by reaction 14, yields a surprising variety of fragments. Although no single CID process is dominant, process 34 dominates at low kinetic energy with process 36 dominating at high kinetic energy.

$$CoFeCp_2C_4H_4^+ \left\{ \begin{array}{ll} \rightarrow CoFeCp_2^+ + C_4H_4 & (31) \\ \rightarrow CoCp_2C_4H_4^+ + Fe & (32) \\ \rightarrow CoCp_2C_4H_2^+ + (FeH_2) & (33) \\ \rightarrow CoFeC_8H_8^+ + C_6H_6 & (34) \\ \rightarrow CoFeC_8H_6^+ + (C_6H_8) & (35) \\ \rightarrow CoCp_2^+ + (FeC_4H_4) & (36) \\ \rightarrow FeCp_2^+ + (CoC_4H_4) & (37) \\ \rightarrow CoC_8H_8^+ + (FeC_6H_6) & (38) \\ \rightarrow CoC_8H_6^+ + (FeC_6H_8) & (39) \\ \rightarrow FeC_8H_6^+ + (CoC_6H_8) & (40) \\ \rightarrow CoC_6H_6^+ + (FeC_8H_8) & (41) \end{array} \right.$$

Processes 31–34 appear to be low-energy decompositions with processes 36–41 occurring for the most part only at high energy. The CID spectra of $Fe_2Cp_2C_4H_4^+$, formed by reaction 14, are considerably simpler than those for $CoFeCp_2C_4H_4^+$ with processes 42–46 observed. Processes

$$Fe_2Cp_2C_4H_4^+ \left\{ \begin{array}{ll} \rightarrow Fe_2Cp_2C_4H_2^+ + H_2 & (42) \\ \rightarrow Fe_2Cp_2^+ + C_4H_4 & (43) \\ \rightarrow FeCp_2C_4H_4^+ + Fe & (44) \\ \rightarrow FeCp_2C_4H_2^+ + (FeH_2) & (45) \\ \rightarrow FeCp_2^+ + (FeC_4H_4) & (46) \end{array} \right.$$

42 and 43 account for more than 60% of the fragmentations at all kinetic energies with the greatest dominance at high energy. $NiFeCp_2C_4H_4^+$, generated by reaction of $NiC_4H_6^+$ with ferrocene (process 14), undergoes reactions 47–53 upon collisional activation. All of these processes occur to a significant extent with processes 51–53 being more dominant at high energy.

Decomposition of $CoNiCp_2C_4H_4^+$, produced by reaction 15, following collisional activation yields reactions 54–59.

---

[18] This reaction has previously been observed. See ref 17b.

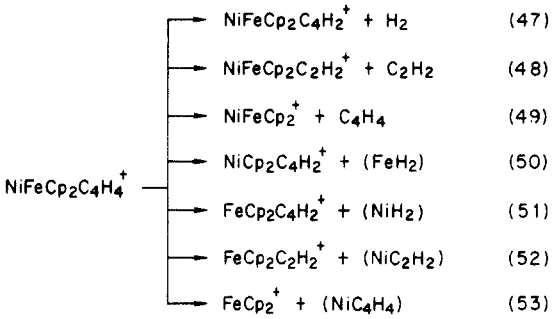

$$NiFeCp_2C_4H_4^+ \rightarrow NiFeCp_2C_4H_2^+ + H_2 \quad (47)$$
$$\rightarrow NiFeCp_2C_2H_2^+ + C_2H_2 \quad (48)$$
$$\rightarrow NiFeCp_2^+ + C_4H_4 \quad (49)$$
$$\rightarrow NiCp_2C_4H_2^+ + (FeH_2) \quad (50)$$
$$\rightarrow FeCp_2C_4H_2^+ + (NiH_2) \quad (51)$$
$$\rightarrow FeCp_2C_2H_2^+ + (NiC_2H_2) \quad (52)$$
$$\rightarrow FeCp_2^+ + (NiC_4H_4) \quad (53)$$

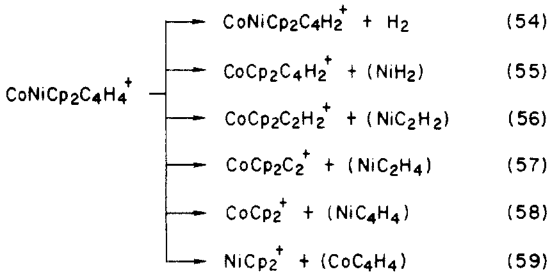

$$CoNiCp_2C_4H_4^+ \rightarrow CoNiCp_2C_4H_2^+ + H_2 \quad (54)$$
$$\rightarrow CoCp_2C_4H_2^+ + (NiH_2) \quad (55)$$
$$\rightarrow CoCp_2C_2H_2^+ + (NiC_2H_2) \quad (56)$$
$$\rightarrow CoCp_2C_2^+ + (NiC_2H_4) \quad (57)$$
$$\rightarrow CoCp_2^+ + (NiC_4H_4) \quad (58)$$
$$\rightarrow NiCp_2^+ + (CoC_4H_4) \quad (59)$$

CID of $CoNiCp_2C_4H_2^+$ yields similar products. In both cases, formation of $CoCp_2C_4H_2^+$ is by far the dominant process accounting for more than 60% of the fragmentations at all kinetic energies. Collisional activation of $CoCp_2C_4H_2^+$, formed by process 55, yields no fragmentations indicating that it is quite stable.

Collisional activation of $Ni_2Cp_2C_4H_4^+$, produced by reaction 15, results in the fragmentations shown in eq 60–64.

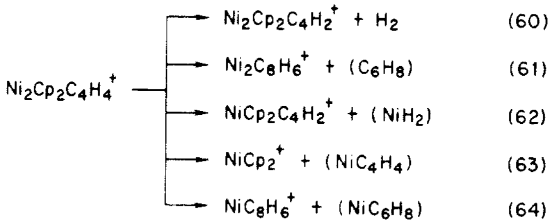

$$Ni_2Cp_2C_4H_4^+ \rightarrow Ni_2Cp_2C_4H_2^+ + H_2 \quad (60)$$
$$\rightarrow Ni_2C_8H_6^+ + (C_6H_8) \quad (61)$$
$$\rightarrow NiCp_2C_4H_2^+ + (NiH_2) \quad (62)$$
$$\rightarrow NiCp_2^+ + (NiC_4H_4) \quad (63)$$
$$\rightarrow NiC_8H_6^+ + (NiC_6H_8) \quad (64)$$

Process 60 dominates at low collision energy while process 61 dominates at high collision energy. CID of $Ni_2Cp_2C_4H_2^+$, generated by reaction 16, yields predominantly formation of $NiCp_2C_4H_2^+$ with some $Ni_2C_8H_6^+$ and $NiC_8H_6^+$ also observed.

Decomposition of $M'M_nCp_m^+$ ($n = 2, 3$; $m = 3, 4$). $Ni_3Cp_4^+$ and $Fe_3Cp_4^+$, generated in reactions 17 and 18, eliminate the corresponding metallocene in high efficiency upon collisional activation (process 65). At high kinetic

$$M_3Cp_4^+ \rightarrow M_2Cp_2^+ + MCp_2 \quad (65)$$

energy nickelocene and ferrocene ions are also observed. CID of $NiFe_2Cp_4^+$, generated in reaction 24, yields elimination of ferrocene in high efficiency (process 66). At high

$$NiFe_2Cp_4^+ \rightarrow NiFeCp_2^+ + FeCp_2 \quad (66)$$

energy formation of $FeCp_2^+$ dominates undoubtedly from the subsequent dissociation of $NiFeCp_2^+$. No formation of $Fe_2Cp_2^+$ is observed at any kinetic energy. The CID spectra of $CoFe_2Cp_4^+$, generated in reaction 27, are similar to those for $NiFe_2Cp_4^+$ with elimination of ferrocene dominating at low energy (process 67). At high energy formation of $FeCp_2^+$ and $CoCp_2^+$ are also observed.

$$CoFe_2Cp_4^+ \rightarrow CoFeCp_2^+ + FeCp_2 \quad (67)$$

Both $Ni_2Cp_3^+$ and $Fe_2Cp_3^+$, generated in reactions 22 and 23, decompose upon collisional activation by eliminating MCp in low efficiency (process 68). CID of $Ni_2Cp_3^+$

$$M_2Cp_3^+ \rightarrow MCp_2^+ + MCp \quad (68)$$

and $Fe_2Cp_3^+$, generated in reactions 69 and 70, yield identical results to that for CID of $Ni_2Cp_3^+$ and $Fe_2Cp_3^+$ formed in reactions 22 and 23.[19]

$$NiCp^+ + NiCp_2 \rightarrow Ni_2Cp_3^+ \quad (69)$$

$$FeCp^+ + FeCp_2 \rightarrow Fe_2Cp_3^+ \quad (70)$$

Discussion

The metal-switching reactions 7 and 12 must proceed by elimination of MC_4H_8 and MC_4H_6 rather than by sequential elimination of the ligand and the metal, since elimination of a metal atom and either isobutene or butadiene is calculated to be endothermic.[4,20] Observation of the charge-transfer reactions 8 and 13 imply $IP(MC_4H_8)$ and $IP(MC_4H_6)$ exceed $IP(FeCp_2) = 6.88$ eV[4] for M = Fe, Co, and Ni.[21] This, coupled with the M^+–L bond energies[20] yields the following limits for D(M–L): $D(Fe–C_4H_8) > 18$ kcal/mol, $D(Co–C_4H_8) > 18$ kcal/mol, $D(Ni–C_4H_8) > 23$ kcal/mol, $D(Fe–C_4H_6) > 28$ kcal/mol, $D(Co–C_4H_6) > 28$ kcal/mol, and $D(Ni–C_4H_6) > 33$ kcal/mol.[4,20] An error of ±6 kcal/mol for the M^+–L bond energies also applies to the above limits.

Observation of reaction 11 implies that the binding energies of Fe^+, Co^+, and Ni^+ to ferrocene and nickelocene exceed 50 ± 5 kcal/mol.[20] This, combined with the heats of formation for $MCp_2(g)$,[22] yields upper limits for $\Delta H_f°(M'MCp_2^+)$ of 286 kcal/mol for $Fe_2Cp_2^+$, 308 kcal/mol for $Ni_2Cp_2^+$, 287 kcal/mol for $CoFeCp_2^+$, 284 kcal/mol for $FeNiCp_2^+$, and 312 kcal/mol for $CoNiCp_2^+$. An error of ±5 kcal/mol on these values carries over.

The ionization potentials (IP) of the mixed-metal metallocenes can be bracketed by monitoring charge-transfer reactions.[21] Reactions 25 and 65 imply 5.56 eV < $IP(Fe_2Cp_2)$ < 6.88 eV, reactions 20 and 66 imply 6.51 eV < $IP(FeNiCp_2)$ < 6.88 eV, reactions 26 and 67 imply $IP(CoFeCp_2) \approx 6.51$ eV, reactions 19 and 65 imply 5.56 eV < $IP(Ni_2Cp_2)$ < 6.51 eV, and lack of charge exchange with $NiCp_2$ suggests $IP(CoNiCp_2)$ < 6.51 eV.[4] These results together with the limits for $\Delta H_f°$ $(M'MCp_2^+)$ yield the following upper limits for $\Delta H_f°$ of the neutral $M'MCp_2$ species of 142 ± 16 kcal/mol for Fe_2Cp_2, 169 ± 12 kcal/mol for Ni_2Cp_2, 137 ± 6 kcal/mol for $CoFeCp_2$, and 129 ± 8 kcal/mol for $FeNiCp_2$.

Finally, these results yield $D(Fe–FeCp_2) > 13 \pm 16$ kcal/mol, $D(Ni–NiCp_2) > 14 \pm 12$ kcal/mol, $D(Co–FeCp_2) > 20 \pm 8$ kcal/mol, $D(Fe–CoCp_2) > 29 \pm 6$ kcal/mol, $D(Fe–NiCp_2) > 50 \pm 7$ kcal/mol, and $D(Ni–FeCp_2) > 29 \pm 8$ kcal/mol.

The $M'MCp_2^+$ ions, generated in reactions 6 and 11, can consist of three general structures, **1**–**3**. Structure **1** is related to the triple-decker compounds (M_2Cp_3) generated in solution with one of the cyclopentadienyl rings miss-

---

[19] These ions have previously been observed in the mass spectra of ferrocene and nickelocene. See, for example: (a) Schumacher, E.; Taubenest, R. *Helv. Chim. Acta* **1964**, *47*, 1525. (b) Hunt, D. F.; Russell, J. W.; Torian, R. L. *J. Organomet. Chem.* **1972**, *43*, 175. (c) Schildcrout, S. M. *J. Am. Chem. Soc.* **1973**, *95*, 3846. (d) Reference 17.

[20] The binding energy of Fe^+, Co^+, and Ni^+ to isobutene and butadiene appears to be in the range of 35–45 and 45–55 kcal/mol, respectively. (a) Armentrout, P. B.; Beauchamp, J. L. *J. Am. Chem. Soc.* **1981**, *103*, 6628. (b) Armentrout, P. B.; Beauchamp, J. L. *J. Am. Chem. Soc.* **1981**, *103*, 784. (c) Halle, L. F.; Armentrout, P. B.; Beauchamp, J. L. *Organometallics* **1982**, *1*, 963. (d) Jacobson, D. B.; Freiser, B. S. *J. Am. Chem. Soc.* **1983**, *105*, 7492. (e) Jacobson, D. B.; Freiser, B. S. *J. Am. Chem. Soc.* **1984**, *106*, 3891.

[21] The preferred ionic product in ion–molecule reactions and ion decompositions is the fragment having the lower IP and is referred to as Stevenson's rule (Stevenson, D. P. *Discuss. Faraday Soc.* **1951**, *10*, 35).

[22] $\Delta H_f°(FeCp_2) = 55.3 \pm 1$ kcal/mol, $\Delta H_f°(CoCp_2) = 66.4 \pm 1$ kcal/mol, and $\Delta H_f°(NiCp_2) = 79.9 \pm 1$ kcal/mol from: Chipperdield, J. R.; Sneyd, J. C. P.; Webster, D. E. *J. Organomet. Chem.* **1979**, *178*, 177.

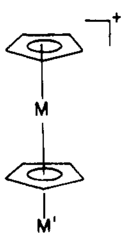

1

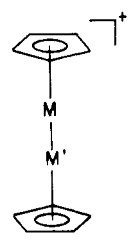

2

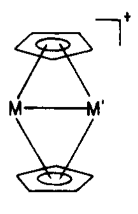

3

ing.[23-25] Observation that CID on $Fe_2Cp_2^+$ formed by 20-eV EI on $[FeCp(CO)_2]_2$ is identical with that for $Fe_2Cp_2^+$ generated in reactions 6 and 11 supports a structure containing a metal–metal bond, either 2 or 3.

Binuclear sandwich-type complexes possessing a metal–metal bonded M_2 unit coordinated by two planar C_nH_n ring systems are very rare.[26] Ozin et al. recently reported the observation of M'M(arene)$_2$ (M', M = Cr, V) species in a frozen matrix by codeposition of the metal with M(arene)$_2$.[27] The data supported a structure more similar to 3 than to 2. Two bridging arene groups have been reported for the compounds $(C_6H_6)_2Pd_2(Al_2Cl_7)_2$[28] and $(C_6H_6)_2Pd_2(AlCl_4)_2$.[29] In addition $(\mu\text{-}C_5H_5)(\text{allyl})M_2L_2$ are known for both Pd[30,31] and Pt[30,32] as well as the "real" bridging sandwich compounds $(\mu\text{-}C_5H_5)_2Pd_2L_2$.[33] Synthesis of the corresponding Ni–Ni species, however, has been unsuccessful.[26] Therefore, the bridging structure 3 has precendent in solution-phase studies. Some form of structure 3 seems more reasonable than the linear structure 2. The actual structure may consist of an unsymmetrical arrangement with the cyclopentadienyl groups biased toward one of the metals. The CID results for $^{58}Ni^{60}NiCp_2^+$, generated in reaction 29, support a mechanism where the two nickel atoms can become equivalent, in either structure 2 or structure 3. For both $CoNiCp_2^+$ and $FeNiCp_2^+$, the structure may actually consist of cobaltocene and ferrocene cations perturbed by the presence of a nickel atom rather than a true bridging structure as in 3.

CID of $CoNiCp_2C_4H_4^+$, $CoNiCp_2C_4H_2^+$, $Ni_2Cp_2C_4H_4^+$, and $Ni_2Cp_2C_4H_2^+$ yield predominantly formation of $MCp_2C_4H_2^+$ species. Absence of fragmentations for collisional activation of $CoCp_2C_4H_2^+$ indicates formation of a very stable species. These ions may consist of a structure where the two Cp rings are bridged by the C_4 unit such as 4. Ring bridges are known for several metallocenes.[34-36]

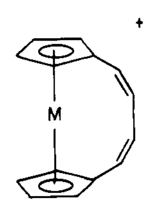

4

The variety of CID processes for the $M'MCp_2C_4H_4^+$ ions makes interpretation of the results difficult and quite speculative. It appears, however, that the cyclopentadienyl rings may incorporate some of the carbons of the C_4H_4 unit upon collisional activation. For example, $CoFeC_8H_8^+$ (formed in process 34) may consist of cyclooctatetraene bridging the two metal centers. Both $C_8H_8Fe_2(CO)_5$ and $C_8H_8Co_2(CO)_4$ contain an M–M unit bridged by cyclooctatetraene.[37-39] In addition the binuclear sandwich compound, $(C_8H_8)_2Ni_2$ has been synthesized and found to contain two nickel atoms bridged by the cyclooctatetraene ligands. The Ni–Ni distance, however, seems too long for a direct metal–metal bond.[39] $CoFeC_8H_6^+$ (process 35) and $Ni_2C_8H_6^+$ (process 61) may consist of the two metals bound to cycloocta-3,5,7-trien-1-yne. Stable benzyne complexes have been reported for nickel,[40] tantalum,[41] and niobium.[41]

The $Ni_2Cp_3^+$ and $Fe_2Cp_3^+$ ions generated in reactions 22 and 23 may consist of triple-decker sandwich structures.[24] This structure seems unlikely in the gas phase, however, considering that the charge-exchange reaction (71) does not proceed through a symmetrical intermediate

$$\mathrm{MCp^+ + MCp_2 \rightarrow MCp_2^+ + MCp} \qquad (71)$$

for M = Fe and Ni.[17] This may be due to the absence of lattice effects in the gas phase. These $M_2Cp_3^+$ ions probably consist of a structure containing a metal–metal bond with the three cyclopentadienyl rings situated around the M–M unit.

Although quadruple-decker compounds are known,[42] the $M_3Cp_4^+$ and $M'M_2Cp_4^+$ ions generated in reactions 17, 18, 24, and 27 are not believed to consist of this highly symmetrical structure. The CID results suggest that the initial $M'MCp_2^+$ unit maintains its integrity with the added metallocene coordinated loosely to the $M'MCp_2^+$ unit.

Acknowledgment is made to the Division of Chemical Sciences in the Office of Basic Energy Sciences in the United States Department of Energy (DE-AC02-80ER10689) for supporting this research and to the National Science Foundation (CHE-8310039) for continued support of FTMS methodology.

Registry No. $FeCp_2$, 102-54-5; $NiCp_2$, 1271-28-9.

---

(23) (a) Werner, H.; Salzar, S. *Angew. Chem., Int. Ed. Engl.* **1972**, *11*, 930. (b) Salzer, A.; Werner, H. *Synth. Inorg. Met.-Org. Chem.* **1972**, *2*, 239. (c) Court, T. L.; Werner, H. *J. Organomet. Chem.* **1974**, *65*, 245. (d) Werner, H. *Angew. Chem., Int. Ed. Engl.* **1977**, *16*, 1. (e) Siebert, W. *Nachr. Chem., Tech. Lab.* **1977**, *25*, 597.

(24) Dubler, E.; Textor, M.; Oswald, H. P.; Salzar, A. *Angew. Chem., Int. Ed. Engl.* **1974**, *13*, 135.

(25) Lauher, J. W.; Eliam, M.; Summerville, R. H.; Hoffmann, R. *J. Am. Chem. Soc.* **1976**, *98*, 3219.

(26) Werner, H. *Adv. Organomet. Chem.* **1981**, *19*, 155.

(27) (a) Ozin, G. A.; Francis, C. G.; Huber, H. X.; Andrews, M.; Nazar, L. *J. Am. Chem. Soc.* **1981**, *103*, 2453. (b) Ozin, G. A.; Andrews, M. *Angew. Chem., Int. Ed. Engl.* **1982**, *21*, 212. (c) Ozin, G. A.; Andrews, M. *Angew. Chem. Suppl.* **1982**, 381.

(28) Allegra, G.; Aimmirzi, A.; Porri, L. *J. Am. Chem. Soc.* **1965**, *87*, 1394.

(29) Allegra, G.; Casagrande, A. T.; Immirzi, L.; Porri, L.; Vitulli, G. *J. Am. Chem. Soc.* **1970**, *92*, 289.

(30) (a) Werner, H.; Tune, D.; Parker, G.; Kruger, C.; Brauer, D. J. *Angew. Chem., Int. Ed. Engl.* **1975**, *14*, 185. (b) Kuhn, A.; Werner, H. *J. Organomet. Chem.* **1979**, *179*, 421.

(31) (a) Werner, H.; Kuhn, A.; Tune, D.; Kruger, C.; Brauer, D. J.; Sekutowski, J. C.; Tsay, Y.-H. *Chem. Ber.* **1977**, *110*, 1763. (b) Werner, H.; Kraus, H. J. *Chem. Ber.* **1980**, *113*, 1072.

(32) (a) Werner, H.; Kuhn, A.; Burschka, C. *Chem. Ber.* **1980**, *113*, 2291. (b) Werner, H.; Kuhn, A. *Angew. Chem., Int. Ed. Engl.* **1977**, *16*, 412.

(33) (a) Werner, H.; Kraus, H. J. *J. Chem. Soc., Chem. Commun.* **1979**, 814. (b) Werner, H.; Kraus, H. J. *Angew. Chem., Int. Ed. Engl.* **1979**, *18*, 948.

(34) (a) Rinehart, K. L.; Frerichs, A. K.; Kittle, P. A.; Westman, L. F.; Gustafson, D. H.; Pruett, R. L.; Mc Mahon, J. E. *J. Am. Chem. Soc.* **1960**, *82*, 4111. (b) Laing, M. B.; Trueblood, K. N. *Acta. Crystallogr.* **1965**, *19*, 373.

(35) (a) Hillman, M.; Gordon, B.; Weiss, A. J.; Guzikowski, A. P. *J. Organomet. Chem.* **1978**, *155*, 77. (b) Lentzner, H. L.; Watts, W. E. *J. Chem. Soc. D* **1970**, 26.

(36) (a) Eilbracht, P. *Chem. Ber.* **1976**, *109*, 3136. (b) Eilbracht, P.; Mayser, U.; Tiedtke, G. *Chem. Ber.* **1980**, *113*, 1420.

(37) Fleischer, E. B.; Stone, A. L.; Dewar, R. B. K.; Wright, D. J.; Keller, C. E.; Pettit, R. *J. Am. Chem. Soc.* **1966**, *88*, 3158.

(38) Kitamura, T.; Joh, T. *J. Organomet. Chem.* **1974**, *65*, 235.

(39) Brauer, D. J.; Kruger, C. *J. Organomet. Chem.* **1976**, *122*, 265.

(40) Gowling, E. W.; Kettle, S. F. A.; Sharples, G. M. *Chem. Commun.* **1968**, 21.

(41) McLain, S. J.; Schrock, R. R.; Sharp, P. R.; Churchill, M. R.; Youngs, W. J. *J. Am. Chem. Soc.* **1979**, *101*, 263.

(42) Seibert, W.; Bohle, C.; Kruger, C.; Tsay, Y.-H. *Angew. Chem., Int. Ed. Engl.* **1978**, *17*, 527.